NIH Public Access
Author Manuscript
ACS Nano. Author manuscript; available in PMC 2013 March 27.

Published in final edited form as:
ACS Nano. 2012 March 27; 6(3): 2558–2565. doi:10.1021/nn205023w.

Multifunctional Nanocapsules for Simultaneous Encapsulation of Hydrophilic and Hydrophobic Compounds and On-Demand Release

Shang-Hsiu Hu[1], **San-Yuan Chen**[1,*], and **Xiaohu Gao**[2,*]

[1]Dept. of Materials Sciences and Engineering, National Chiao Tung University, Hsinchu, Taiwan

[2]Department of Bioengineering, University of Washington, Seattle, Washington 98195, U.S.A

Abstract

Cocktail therapy by delivering multiple drugs to diseased cells can elicit synergistic therapeutic effects and better modulate the complex cell signaling network. Besides selection of drug combinations, a difficulty in delivery is how to encapsulate drugs with various solubility into a common vehicle, particularly when both hydrophobic and hydrophilic compounds are involved. Furthermore, it is highly desirable that the drug release profile can be controlled in an on-demand fashion for balanced therapeutic and side effects. Based on a simple and scalable double-emulsion approach, we report a new class of nanocapsules that can solve these problems simultaneously. Further linking the nanocapsules with peptides targeting cell surface integrins leads to significantly enhanced cell uptake of the nanocapsules. Intracellular drug release triggered by external stimuli has also been achieved without affecting cell viability. Further development of this technology should open exciting opportunities in treating tough diseases such as cancer, cardiovascular diseases, neurological disorders, and infectious diseases.

Keywords

Nanocapsule; drug encapsulation; multifunctional; targeted; controlled release

Recent advance in nanotechnology has produced a number of drug delivery systems based on biodegradable polymers, micelles, liposomes, and inorganic nanoparticles for improved therapeutic efficacy and reduced side effect. The versatility and flexibility of these delivery vehicles in drug selection also allow simultaneous encapsulation of multiple types of drug for cocktail therapy. Due to the molecular complexity of many diseases (in particular cancer, cardiovascular diseases, neurological disorders, malaria, and AIDS), smart combination of drugs can better modulate cell signaling network to maximize therapeutic effect and reduce drug resistance.[1–5] For example, it has been shown that co-delivery of paclitaxel and interleukin-12-encoded plasmid using self-assembled polymeric nanoparticles can suppress breast tumor growth in a mouse model more efficiently than the delivery of either compound alone.[6] Similarly, an upsurge of recent reports has demonstrated clear evidence of synergistic effects between chemotherapy drugs and siRNA and reduced multidrug resistance.[7–10] Most recently, Ashley *et al* improved the loading capacity of cocktail drugs by coating mesoporous silica with lipid bilayers to an unprecedented level that a single NP is sufficient to kill a cancer cell.[11]

sanyuanchen@mail.nctu.edu.tw; and xgao@u.washington.edu.

NIH-PA Author Manuscript
NIH-PA Author Manuscript
NIH-PA Author Manuscript

NIH-PA Author Manuscript

NIH-PA Author Manuscript

NIH-PA Author Manuscript

Despite these recent advances in nanocarrier engineering, technological challenges (in addition to the biological challenges such as identification of appropriate drug combination and dosing) in encapsulating multiple therapeutic compounds in one NP still exist. First, it is often difficult to find a common solvent for drugs of different solubilities and a common carrier matrix compatible with all the ingredients in a drug cocktail, particularly when both hydrophobic compounds (*e.g.*, many chemotherapeutic drugs) and hydrophilic materials (*e.g.*, biologics) are involved. In this regard, a popular approach is double emulsion, based on which nanoparticles with compartmentalized internal structure for both polar and non-polar drugs can be made.[12] For example, using double emulsion methods, Woodrow *et al* have encapsulated siRNA molecules in biodegradable hydrophobic polymers for controlled and sustained release of siRNA to vaginal mucosa,[13] whereas Shi and coworkers have shown outstanding siRNA loading efficiency in biodegradable polymer shells by a clever selection of double emulsion surfactants (a positively charged lipid layer for formation of hollow inner core and strong interaction with negatively charged siRNA, and a neutral lipid layer to stabilize the overall NP).[14] The second technological difficulty stems from the kinetics of drug release. In most cases, this process is determined by the degradation rate of the carrier matrix or the diffusion rate of therapeutic compounds, rendering the tunability of drug release profile highly limited. In light that virtually all therapeutic compounds have their own optimal concentration window: too much may lead to elevated side effects whereas too little is insufficient to kill diseased cells, precise control of drug release profile independent of drug and carrier properties can open exciting new opportunities for treatment of tough diseases. In this context, here, we report a new class of nanocapsules (NCs) prepared with a simple, versatile, and scalable double emulsion procedure with remotely controlled drug-release profile.

RESULTS AND DISCUSSION

Synthesis and characterization of nanocapsules

As schematically illustrated in Figure 1a, our procedure employs water-in-oil-in-water (W/O/W) double emulsion for encapsulating both hydrophilic and hydrophobic compounds. In the first step, aqueous solution of hydrophilic compounds (in this study dye-labeled plasmid DNA or water-soluble quantum dots as models) is emulsified with oleic acid as the surfactant in chloroform containing a polymer matrix (poly(styrene-ally alcohol), PS_{16}-PAA_{10}, m.w. 2,200) and hydrophobic dopants such as pyrene dyes and magnetic nanoparticles (MNPs). Previously, MNPs have been used in magnetic separation, biomedical imaging, hyperthermia, and magnetolytic treatment, depending on the strength and frequency of external magnetic fields;[15, 16] and here they serve as an actuator for remotely controlled drug release. Inside alternating magnetic fields of proper frequency, MNPs can quickly heat up the surrounding environment, resulting in deformation of drug carriers or promoted drug diffusion.[17–24] Due to better tissue penetration depth compared with light and heat, magnetic field actuation has become a very attractive mechanism for large-animal and potentially clinical uses.[25] In the second step of the W/O/W double emulsion, although the polymer matrix PS_{16}-PAA_{10} has an amphiphilic nature, it is insufficient to emulsify the organic solvent to form compact and uniform particles, and thus chloroform is emulsified in a water continuous phase with polyvinyl alcohol (PVA, m.w. 9,000) as the surfactant. The organic phase is then slowly evaporated leading to solidification of the NC shell.

The structures of the resulting nanocapsules are thoroughly characterized with transmission electron microscopy (TEM) and dynamic light scattering (DLS). As shown in Fig. 1b, the particles are well dispersed and uniform with an average diameter of approximately 260 nm. Due to the nature of emulsion approach, the nanoparticles are not absolutely monodisperse (standard deviation 30 nm). But interestingly, they share very similar internal structures,

NIH-PA Author Manuscript

NIH-PA Author Manuscript

NIH-PA Author Manuscript

where the aqueous compartment and hydrophobic polymer phase are located on the opposite sides of the NCs with majority of the MNPs sandwiched in between. Although oleic acid-coated MNPs and PS_{16}-PAA_{10} are both hydrophobic, they clearly exhibit phase separation upon solvent evaporation, similar to immiscible polymer blends.[26] In chloroform, oleic acid-coated MNPs have significantly lower solubility than that of PS_{16}-PAA_{10}. Thus, as chloroform evaporates, MNPs precipitate out first and form clusters, followed by solidification of the polymer matrix.[16] The NC size distribution of the resulting double emulsion nanoparticles is also confirmed by dynamic light scattering (DLS) measurements. Figure 1d displays a hydrodynamic diameter of 263 ± 42 nm for the same batch of particles, confirming excellent colloidal dispersity in aqueous solution without the need of additional surfactants, stabilizers, or surface modifications. Compared with the dry size measured with TEM, the DLS size is slightly bigger, likely due to polymer swelling and the hydration layers on nanoparticle surface.

To probe the structural tunability of the double emulsion nanoparticles, we varied the quantity of MNPs and oleic acid in the initial stock solutions while keeping the polymer concentration constant. TEM images in Figure 2 clearly reveal a size increase of the water reservoir as MNP and oleic acid concentration increases. As the weight ratio of MNP/polymer increases from 3.7 to 30%, the size and size distribution of the overall double emulsion particles remain approximately unchanged (Table 1). Further increase the ratio to 60% leads to formation of polydispersed NCs. Despite this qualitative correlation between the initial MNP and oleic acid concentrations and the final water compartment size inside the nanocomposites, the exact volume of the water compartment is difficult to determine due to its non-spherical shape.

Drug encapsulation and release

Next, we investigated the drug encapsulating capacity of the NCs using FITC-labeled plasmid DNA and pegylated quantum dots (QDs) as model water-soluble compounds and pyrene for hydrophobic payload. As shown in Figure 3a, the encapsulation efficiency (EE) of the hydrophilic compounds (both DNA and QDs) gradually increases with the size of the water compartment and peaks above 60%. Similar experiment performed with small-molecule drug, doxorubicin, results in lower EE (20–53% for the same set of NCs), likely due to faster diffusion of small molecules out of the NC either during the emulsion process or after NC formation. The EE of hydrophobic compounds is generally high, ranging between 65% and 95% for this set of samples. Due to the low water-solubility of the pyrene molecules, once encapsulated, they remain in the NCs for months with low level of leaking. In contrast, the release rate of the water-soluble compounds, FITC-DNA, is relatively low but appreciable, likely regulated by the polymer shell. As shown in Figure 3b, in the absence of magnetic induction, the NCs only release 7–25% of the encapsulated DNA over a period of 2 days for the three NC samples studied. This slow release profile could find important uses in sustained drug release. On the other hand, it will be difficult to tune for different drugs with varying size, solubility, and therapeutic range. In this context, magnetic triggering can be an important mechanism for remotely controlled drug release.[27] Compared with other on-demand drug release mechanisms such as near infrared illumination on plasmonic metallic materials and ultrasound absorption by microparticles, magnetic triggering offers outstanding tissue penetration depth and safety, in addition to the excellent biocompatibility and biodegradability of iron oxide-based nanoparticles.

To demonstrate magnetic field-triggered release, one of the NC samples (B30) with encapsulated DNA was placed in high-frequency magnetic fields (HFMF) of varying strengths (0.8, 1.2, and 2.0 kA/m), because inductive heating of MNPs due to energy absorption and subsequent magnetic relaxation has been well documented and applied towards controlled drug release.[17, 19–23, 28, 29] As shown in Figure 3c, a burst in DNA

NIH-PA Author Manuscript

NIH-PA Author Manuscript

NIH-PA Author Manuscript

release is observed each time the magnetic field is applied and the quantity released seems to be field strength-dependent: the stronger the magnetic field, the more DNA released. A closer examination of the three experiment conditions, however, reveals interesting differences between their release profiles. When the field strength is set at 0.8 or 1.2 kA/m, the NCs' drug release follows a burst-to-zero-to-burst staircase-shaped profile, indicating that the thermally accelerated release is a reversible process. Likely, local inductive heating changes the permeability of the hydrophobic shell and the diffusion rate of the encapsulated DNA, leading to temporarily enhanced DNA escape. Switching off the magnetic pulse makes the NCs return to their original states resulting in negligible DNA release in short periods (*e.g.*, 5 min between pulses). Indeed, similar reversible drug release due to thermal triggering has been observed in capsule structures made of polyelectrolytes as well as thermo-responsive hydrogels.[18, 29] In comparison, when the magnetic field strength is increased to 2.0 kA/m, a different trait of DNA release is observed, particularly when the field is switched off. The drug release post exposure to magnetic fields is no longer negligible, indicated by a small slope in the release curve during the time interval between magnetic induction pulses. This observation suggests permanent damages occurred to NCs due to the inductive heating, thus upon removal of the field, cargo DNA keeps leaking into the environment. The released DNA molecules were further examined with gel electrophoresis to confirm their original structure. As show in Figure 3d, the mobilities of the original DNA and DNA released from nanocapsules are identical (same molecular weight), indicating that the overall structure of the encapsulated DNA are not affected during the triggered release process.

To quantify the release of hydrophobic molecules, similar experiments in the absence or presence of HFMF were performed for pyrene as well. Without HFMF, less than 5% of the encapsulated pyrene is released even after 10-day incubation, and the low-level release mainly occurs during the first day, likely due to pyrene attached to NC surface or embedded in superficial layers. In the presence of HFMF at high field strength (2.0 kA/m), the pyrene release quickly increases to ~10% with just three pulses. The profiles of pyrene release are generally similar to those of DNA molecules, but the total released quantities are significantly less. Several factors may contribute to this effect. First, pyrene is highly hydrophobic with low water solubility of 0.135 mg/L, favoring its partition in the more hydrophobic NC core. Second, the magnetic nanoparticles are largely located at the interface of the hydrophilic and hydrophobic compartments, and as a consequence, heat generated by the MNPs unlikely will propagate throughout the polymer phase to promote drug diffusion. We expect this issue can be addressed in future designs with MNPs homogeneous distributed in the hydrophobic polymer phase, such as by changing MNP surface ligand or polymer composition to improve MNP-polymer blending.

Cell targeting and intracellular DNA release

Following the systematic characterizations, we further demonstrated cell targeting and intracellular DNA release using the nanocapsules. To link NCs with targeting ligands, their surfaces are modified with carboxylic acid groups for conjugation with streptavidin, followed by incubation with biotinylated RGD peptide targeting integrins, which play important roles in angiogenesis and tumor cell metastasis and has been proposed as therapeutic targets.[30, 31] To evaluate the targeting specificity of the multifunctional NCs, human breast tumor cells, MCF-7, with high expression levels of $\alpha_v\beta_3$ are incubated with NCs with or without the targeting RGD peptide. For comparison, HeLa cells (cervical tumor) with relatively low level of surface $\alpha_v\beta_3$ are used. We have confirmed $\alpha_v\beta_3$ expression of the two cell lines by labeling cells with biotinylated RGD peptide and fluorescently labeled streptavidin. Flow cytometry measurements show that the fluorescence of stained HeLa cells is distinguishable from negative controls but 6–7 times lower than that

NIH-PA Author Manuscript

NIH-PA Author Manuscript

NIH-PA Author Manuscript

of MCF-7 cells (data not shown). After 24-hour incubation with RGD-targeted nanocapsules, highly fluorescent MCF-7 cells (due to the encapsulated FITC-DNA) are observed with confocal fluorescence imaging (Figure 4a). In fact, 4-hour incubation is already sufficient to demonstrate the differential intracellular uptake between MCF-7 cells treated with the RGD-targeted NCs, with the controls including MCF-7 cells treated with non-targeted NCs, HeLa cells treated with targeted or non-targeted NCs. Quantitative flow cytometry studies show fluorescence histograms of the three controls are located around the first log, whereas that of the experiment group is centered around the third log (Fig. 4b), indicating good targeting specificity.

A remaining important issue is whether the magnetically inducible cargo release can be achieved in live cells without causing non-specific cytotoxicity. Below the maximum permissible exposure (MPE) level (*e.g.*, whole-body MPE set by IEEE is kW/cm^2 for 50 kHz, IEEE C95.1-1991), electromagnetic field does not result in serious tissue damage. However, in the presence of superparamagnetic nanoparticles, the field energy can be captured efficiently and converted into heat, which serves as the key mechanism for magnetically triggered drug release and hyperthermia-based therapy.[32] In our study, cell viabilities in the presence of the nanocapsules are only reduced by 3% and 5% before and after the short exposure to the magnetic field (at 2 kA/m), indicating low level of chemical and hyperthermia-induced toxicity of the NCs. This is perhaps not too surprising considering the combination of low NC concentration in cells,[19] short duration of field exposure, and limited heat dissipation beyond nanoparticle surface.[22] To investigate HFMF-induced DNA release, the MCF-7 cells tagged with nanocapsules were exposed to HFMF (2.0 kA/m) for 2 min, followed by a one-hour incubation for DNA release. An approximately 5–6 fold increase of intracellular fluorescence intensity was observed with flow cytometry (Fig. 5a) and confocal microscopy (Fig. 5b), suggesting the escape of FITC-labeled DNA from the NCs. This fluorescence enhancement could be due to reduced quenching and increased pH values. When FITC-DNA molecules are encapsulated in the nanocapsules, partial quenching due to high concentration of the dye molecules (also known as self quenching) and the magnetic nanoparticles (have very broad absorption profile in the visible spectrum) are likely to occur. Elimination of these potential quenching mechanisms by releasing FITC-DNA into cytoplasm results in fluorescence enhancement. In addition, it is also known that the fluorescence of FITC fluctuates with pH, which actually makes FITC a pH sensing material. When FITC-labeled DNA gets released from acidic endosome to cytoplasm, its fluorescence might increase too. To pinpoint the exact mechanisms and quantify their contributions, further quantitative measurements are needed.

CONCLUSION

In summary, we have developed a new class of nanocapsules based on a simple, versatile, and scalable double emulsion approach. The nanocapsules are capable of encapsulating both hydrophobic and hydrophilic compounds at high efficiency. It is worth mentioning another popular strategy for co-delivery of both hydrophilic and hydrophobic compounds: doping small-molecule drugs inside nanoparticles and attach biomacromolecules to nanoparticle surface. For example, Zhu *et al* have prepared biodegradable cationic micelles using A-B-A triblock copolymers with paclitaxel encapsulated inside and siRNA molecules adsorbed to the surface.[10] Similarly, Meng and coworkers recently used mesoporous silica nanoparticles to encapsulate a chemotherapeutic agent and immobilize siRNA molecules targeting efflux transporters to overcome the multiple drug resistance (MDR) in cancer cells.[33] Compared to these designs, encapsulation of biomacromolecules inside could offer improved stability against enzymatic degradation. Besides drug encapsulation, we further show that the nanocapsules are responsive to external magnetic fields for remotely controlled drug release. At low field strengths, the accelerated drug release profile is reversible when the HFMF is

NIH-PA Author Manuscript

NIH-PA Author Manuscript

NIH-PA Author Manuscript

turned off, whereas high field strengths can permanently damage NCs, leading to cargo release in the absence of HFMF. This field strength-dependent behavior offers a sharper response compared with nanocapsules responding to pH and temperature changes,[34] and can be potentially used for precise control of optimal therapeutics' concentration. We were also able to functionalize the NCs with RGD peptides for specific cell targeting through surface integrins and to probe the possibility of intracellular cargo release. With short exposure to HFMF, the cell viability is virtually unaffected, but the cargo release can be readily detected by flow cytometry and confocal microscopy. Further development and optimization of this technology can lead to new opportunities for cocktail therapy in particular when both hydrophobic and hydrophilic compounds are involved.

MATERIALS AND METHODS

Unless specified, chemicals were purchased from Sigma-Aldrich (St. Louis, MO) and used without further purification. FITC-labeled plasmid DNA (Label IT® Plasmid, 2.7 kb) was purchased from Mirus (Madison, WI).

Synthesis of nanocapsules via double emulsion

Under pulsed sonication, water-in-oil (W/O) emulsion was carried out by emulsifying 100 μL aqueous phase in 500 μL PS_{16}-b-PAA_{10} (m.w. 2,200 g/mol) polymer solution (chloroform, organic phase) in the presence of oleic acid as the surfactant. For cargo encapsulation, water-soluble compounds such as FITC-DNA or fluorophores were included in the aqueous phase in advance, and hydrophobic compounds such as pyrene were added to the polymer solution. The W/O emulsion was then added to another aqueous continuous phase (2 mL) in the presence of PVA (m.w. 9–10k, 2%), and emulsified again with pulsed sonication. The specific amounts of the regents are listed in Table 1. The W/O/W double emulsion was stirred at room temperature for 24 hours to evaporate the organic solvent. The resulting nanocapsules were washed with D.I. water for 3 times.

Bioconjugation of nanocapsules with RGD peptide

To add a small percentage of reactive carboxylic acid groups to the PVA surface, the alkylation protocol developed by Weissleder *et al* was adopted with minor adjustments.[35] Briefly, bromoacetic acid in water (1 wt%) was added dropwise to nanocapsules (0.5 g) dispersed in sodium hydroxide (0.05 g) water solution (10 mL). The mixture was stirred overnight at room temperature and neutralized with hydrochloric acid. After washing, the nanocapsules with reactive carboxylic surface groups were activated with 0.4 M EDAC (1-Ethyl-3-[3- dimethylaminopropyl] carbodiimide hydrochloride) and 0.1 M NHS (N-Hydroxysuccinimide) for 30 min (pH 4.5). The activated beads were then quickly isolated and incubated with streptavidin (0.1 mg/mL). After purification, cRGD-PEG_2-biotin (Peptides International, Inc., USA) was linked to the nanocapsules through the strong streptavidin-biotin interaction.

Efficiency of drug loading and release

Hydrophilic compounds such as FITC-labeled pDNA, QDs, and pyrene were used as models, with initial concentrations kept at 5 μg/ml, 3.4 nM, and 0.135 mg/L, respectively. To assess the loading efficiency of the synthesized NCs, the fluorescent compounds left in the supernatant were quantified after removing the nanocapsules by centrifugation. All measurements were performed in triplicates. The encapsulation efficiency was calculated by taking the ratio of (total amount of drug – drug remaining in the supernatant) over the total amount of drug. The drug release profile is studied in the same way by spinning down the nanocapsules and measuring fluorescence intensity of the supernatants. For magnetically triggered release, high frequency magnetic fields (HFMF, 50 kHz) of various field strengths

NIH-PA Author Manuscript

NIH-PA Author Manuscript

NIH-PA Author Manuscript

were applied to DNA-loaded nanocapsules. The HFMF inductive heating system consisted of a power supply, function generator, amplifier, and a water-cooled (cooling water temperature 25 °C) coil of 8 loops. This system offers variable magnetic field strengths in the center of the coil between 0 and 2.5 kA/m. Similar HFMF setup can be found in previously published work.[36]

Cell culture

HeLa (human cervical cancer) and MCF-7 (breast cancer) cells were maintained in DMEM (Dulbecco's modified Eagle's medium) containing 10% fetal bovine serum, 100 units/mL penicillin, and 100 μg/mL streptomycin. Cells were maintained at 37 °C in a humidified atmosphere with 5% CO_2. Nanocapsule cellular uptake was observed on a confocal microscope (Nikon C1) and quantitatively measured on a flow cytometer (BD FACSCalibur).

Cytotoxicity characterization

Standard MTT assay was performed to determine the effect of the magnetic fields and the nanocapsules. Briefly, cells were seeded at a density 10,000 cells/well in 96-well flat-bottomed microtiter plates. After exposure to NCs and magnetic fields as described above, the cells were incubated with 20 μl MTT solution for 4 hours. The media were then replaced with 200 μl DMSO for absorption measurement with a plate reader.

Acknowledgments

This work was supported in part by grants to X.H.G from NIH (R01CA131797, R01CA140295), NSF (0645080), and the UW, to S.Y.C from National Science Council of the Republic of China, Taiwan under Contract of NSC99-2221-E-009-070-MY3 and NSC100-2320-B-009-006-MY2. S.H.H. thanks National Science Council of Taiwan for a study abroad fellowship. We are also grateful to UW-NTUF for TEM and SEM, and Dr. Y.A. Wang at Oceannanotech for the uniform MNPs.

References

1. Greco F, Vicent MJ. Combination Therapy: Opportunities and Challenges For Polymer-Drug Conjugates as Anticancer Nanomedicines. Adv Drug Del Rev. 2009; 61:1203–1213.
2. Lane D. Designer Combination Therapy for Cancer. Nat Biotechnol. 2006; 24:163–164. [PubMed: 16465160]
3. Lebedeva IV, Washington I, Sarkar D, Clark JA, Fine RL, Dent P, Curiel DT, Turro NJ, Fisher PB. Strategy for Reversing Resistance to A Single Anticancer Agent in Human Prostate and Pancreatic Carcinomas. Proc Nat Acad Sci US A. 2007; 104:3484–3489.
4. Rubinfeld B, Upadhyay A, Clark SL, Fong SE, Smith V, Koeppen H, Ross S, Polakis P. Identification and Immunotherapeutic Targeting of Antigens Induced by Chemotherapy. Nat Biotech. 2006; 24:205–209.
5. Sengupta S, Eavarone D, Capila I, Zhao G, Watson N, Kiziltepe T, Sasisekharan R. Temporal Targeting of Tumour Cells and Neovasculature with A Nanoscale Delivery System. Nature. 2005; 436:568–572. [PubMed: 16049491]
6. Wang Y, Gao S, Ye WH, Yoon HS, Yang YY. Co-Delivery of Drugs and DNA from Cationic Core-Shell Nanoparticles Self-Assembled from A Biodegradable Copolymer. Nat Mater. 2006; 5:791–796. [PubMed: 16998471]
7. Chen AM, Zhang M, Wei D, Stueber D, Taratula O, Minko T, He H. Co-Delivery of Doxorubicin and Bcl-2 Sirna by Mesoporous Silica Nanoparticles Enhances The Efficacy of Chemotherapy in Multidrug-Resistant Cancer Cells. Small. 2009; 5:2673–2677. [PubMed: 19780069]
8. Sun TM, Du JZ, Yao YD, Mao CQ, Dou S, Huang SY, Zhang PZ, Leong KW, Song EW, Wang J. Simultaneous Delivery of siRNA and Paclitaxel *via* a "Two-in-One" Micelleplex Promotes Synergistic Tumor Suppression. ACS Nano. 2011; 5:1483–1494. [PubMed: 21204585]

NIH-PA Author Manuscript

NIH-PA Author Manuscript

NIH-PA Author Manuscript

9. Xiong XB, Lavasanifar A. Traceable Multifunctional Micellar Nanocarriers for Cancer-Targeted Co-delivery of MDR-1 siRNA and Doxorubicin. ACS Nano. 2011; 5:5202–5213. [PubMed: 21627074]
10. Zhu C, Jung S, Luo S, Meng F, Zhu X, Park TG, Zhong Z. Co-delivery of SiRNA and Paclitaxel into Cancer Cells by Biodegradable Cationic Micelles Based on PDMAEMA-PCL-PDMAEMA Triblock Copolymers. Biomaterials. 2010; 31:2408–2416. [PubMed: 19963269]
11. Ashley CE, Carnes EC, Phillips GK, Padilla D, Durfee PN, Brown PA, Hanna TN, Liu J, Phillips B, Carter MB, et al. The Targeted Delivery of Multicomponent Cargos to Cancer Cells by Nanoporous Particle-Supported Lipid Bilayers. Nat Mater. 2011; 10:389–397. [PubMed: 21499315]
12. Hanson JA, Chang CB, Graves SM, Li Z, Mason TG, Deming TJ. Nanoscale Double Emulsions Stabilized By Single-Component Block Copolypeptides. Nature. 2008; 455:85–88. [PubMed: 18769436]
13. Woodrow KA, Cu Y, Booth CJ, Saucier-Sawyer JK, Wood MJ, Mark Saltzman W. Intravaginal Gene Silencing Using Biodegradable Polymer Nanoparticles Densely Loaded with Small-Interfering RNA. Nat Mater. 2009; 8:526–533. [PubMed: 19404239]
14. Shi J, Xiao Z, Votruba AR, Vilos C, Farokhzad OC. Differentially Charged Hollow Core/Shell Lipid–Polymer–Lipid Hybrid Nanoparticles for Small Interfering RNA Delivery. Angew Chem Int Ed. 2011; 50:7027–7031.
15. McCarthy JR, Weissleder R. Multifunctional Magnetic Nanoparticles for Targeted Imaging and Therapy. Adv Drug Del Rev. 2008; 60:1241–1251.
16. Hu SH, Gao XH. Nanocomposites with Spatially Separated Functionalities for Combined Imaging and Magnetolytic Therapy. J Am Chem Soc. 2010; 132:7234–7237. [PubMed: 20459132]
17. Brule S, Levy M, Wilhelm C, Letourneur D, Gazeau F, Menager C, Le Visage C. Doxorubicin Release Triggered by Alginate Embedded Magnetic Nanoheaters: A Combined Therapy. Adv Mater. 2010; 23:787–790. [PubMed: 21287643]
18. Choi SH, Lee JH, Choi SM, Park TG. Thermally Reversible Pluronic/Heparin Nanocapsules Exhibiting 1000-Fold Volume Transition. Langmuir. 2006; 22:1758–1762. [PubMed: 16460102]
19. Derfus AM, von Maltzahn G, Harris TJ, Duza T, Vecchio KS, Ruoslahti E, Bhatia SN. Remotely Triggered Release From Magnetic Nanoparticles. Adv Mater. 2007; 19:3932–3936.
20. Hu SH, Chen SY, Liu DM, Hsiao CS. Core/Single-Crystal-Shell Nanospheres for Controlled Drug Release *via* A Magnetically Triggered Rupturing Mechanism. Adv Mater. 2008; 20:2690–2695.
21. Kong SD, Zhang WZ, Lee JH, Brammer K, Lal R, Karin M, Jin SH. Magnetically Vectored Nanocapsules for Tumor Penetration and Remotely Switchable On-Demand Drug Release. Nano Lett. 2010; 10:5088–5092.
22. Liu TY, Liu KH, Liu DM, Chen SY, Chen IW. Temperature-Sensitive Nanocapsules for Controlled Drug Release Caused by Magnetically Triggered Structural Disruption. Adv Func Mater. 2009; 19:616–623.
23. Thomas CR, Ferris DP, Lee JH, Choi E, Cho MH, Kim ES, Stoddart JF, Shin JS, Cheon J, Zink JI. Noninvasive Remote-Controlled Release of Drug Molecules in Vitro Using Magnetic Actuation of Mechanized Nanoparticles. J Am Chem Soc. 2010; 132:10623–10625. [PubMed: 20681678]
24. Timko BP, Dvir T, Kohane DS. Remotely Triggerable Drug Delivery Systems. Adv Mater. 2010; 22:4925–4943. [PubMed: 20818618]
25. Johannsen M, Gneveckow U, Eckelt L, Feussner A, WaldÃ–Fner N, Scholz R, Deger S, Wust P, Loening SA, Jordan A. Clinical Hyperthermia of Prostate Cancer Using Magnetic Nanoparticles: Presentation of A New Interstitial Technique. Inter J Hyperthermia. 2005; 21:637–647.
26. Kietzke T, Neher D, Kumke M, Ghazy O, Ziener U, Landfester K. Phase Separation of Binary Blends in Polymer Nanoparticles. Small. 2007; 3:1041–1048. [PubMed: 17480045]
27. Lobovkina T, Jacobson GB, Gonzalez-Gonzalez E, Hickerson RP, Leake D, Kaspar RL, Contag CH, Zare RN. In Vivo Sustained Release of siRNA from Solid Lipid Nanoparticles. ACS Nano. 2011; 5:9977–9983. [PubMed: 22077198]
28. Hoare T, Santamaria J, Goya GF, Irusta S, Lin D, Lau S, Padera R, Langer R, Kohane DS. A Magnetically Triggered Composite Membrane for On-Demand Drug Delivery. Nano Lett. 2009; 9:3651–3657. [PubMed: 19736912]

NIH-PA Author Manuscript

NIH-PA Author Manuscript

NIH-PA Author Manuscript

29. Lu ZH, Prouty MD, Guo ZH, Golub VO, Kumar CSSR, Lvov YM. Magnetic Switch of Permeability for Polyelectrolyte Microcapsules Embedded with Co@Au Nanoparticles. Langmuir. 2005; 21:2042–2050. [PubMed: 15723509]

30. Ruoslahti E, Pierschbacher MD. ARG-GLY-ASP - A Versatile Cell Recognition Signal. Cell. 1986; 44:517–518. [PubMed: 2418980]

31. Ruoslahti E, Pierschbacher MD. New Perspectives In Cell-Adhesion - RGD and Integrins. Science. 1987; 238:491–497. [PubMed: 2821619]

32. Ahlbom A, Bergqvist U, Bernhardt JH, Cesarini JP, Court LA, Grandolfo M, Hietanen M, McKinlay AF, Repacholi MH, Sliney, et al. Int Commission Nonionizing Radiation, P., Guidelines for Limiting Exposure to Time-Varying Electric, Magnetic, and Electromagnetic Fields (up to 300 GHz). Health Physics. 1998; 74:494–522. [PubMed: 9525427]

33. Meng H, Liong M, Xia T, Li Z, Ji Z, Zink JI, Nel AE. Engineered Design of Mesoporous Silica Nanoparticles to Deliver Doxorubicin and P-Glycoprotein siRNA to Overcome Drug Resistance in a Cancer Cell Line. ACS Nano. 2010; 4:4539–4550. [PubMed: 20731437]

34. Chen W, Meng F, Cheng R, Zhong Z. pH-Sensitive Degradable Polymersomes for Triggered Release of Anticancer Drugs: A Comparative Study with Micelles. J Control Release. 2010; 142:40–46. [PubMed: 19804803]

35. Liong M, Shao H, Haun JB, Lee H, Weissleder R. Carboxymethylated Polyvinyl Alcohol Stabilizes Doped Ferrofluids for Biological Applications. Adv Mater. 2010; 22:5168–5172. [PubMed: 20859943]

36. Mohr R, Kratz K, Weigel T, Lucka-Gabor M, Moneke M, Lendlein A. Initiation of Shape-Memory Effect by Inductive Heating of Magnetic Nanoparticles in Thermoplastic Polymers. Proc Nat Acad Sci US A. 2006; 103:3540–3545.

NIH-PA Author Manuscript

NIH-PA Author Manuscript

NIH-PA Author Manuscript

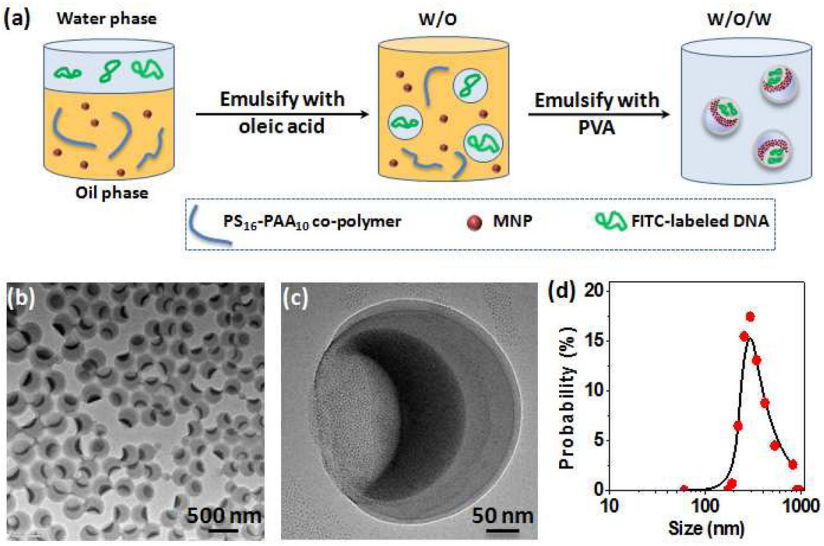

Figure 1.

Nanocapsule synthesis and size characterization. (a) Schematic illustration of the key steps in nanocapsule preparation. In the first step (W/O emulsion), aqueous solution of hydrophilic compounds (*e.g.*, biologics) are emulsified in a volatile organic solvent (in this paper, chloroform) with oleic acid as the surfactant, followed by the second round emulsion (W/O/W) with PVA as the surfactant. (b, c) TEM images of the nanocapsules prepared *via* the double emulsion approach. The scale bars are 500 nm for the low magnification image, and 50 nm for the high magnification image. (d) Hydrodynamic size (263 ± 42 nm) of the nanocapsules measured by DLS.

NIH-PA Author Manuscript
NIH-PA Author Manuscript
NIH-PA Author Manuscript

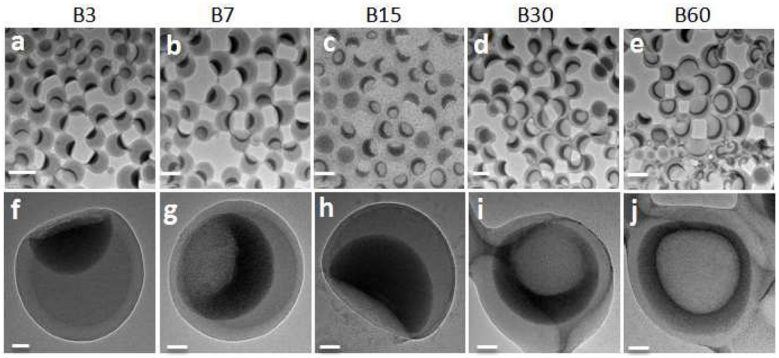

Figure 2.

Nanocapsule size tunability. Increasing the concentrations of MNPs and oleic acid leads to gradual size increase of NCs' inner aqueous compartment. Scale bars: (a–e) 200 nm, and (f–j) 20 nm. Due to the high density of nanoparticles on electron microscopy grid, some of them appear to be connected. This is mainly because of the drying process during sample preparation rather than aggregation in solution, which has been confirmed with DLS measurements (see Table 1).

NIH-PA Author Manuscript
NIH-PA Author Manuscript
NIH-PA Author Manuscript

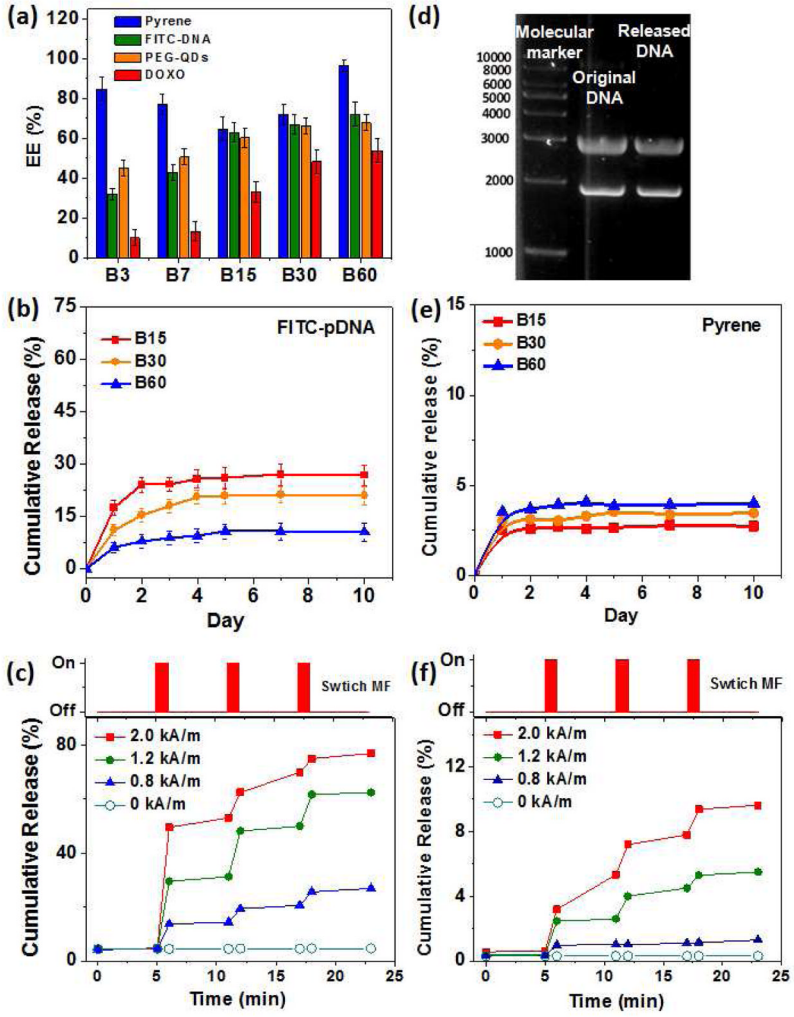

Figure 3.

Characterization of NCs' encapsulation efficiency and cargo release profile. (a) EE for FITC-labeled plasmid DNA, water-soluble quantum dots, doxorubicin, and pyrene. The EE of hydrophobic pyrene are generally high in all the formulations, where as the EE of hydrophilic compounds appears to be dependent on the size of the hydrophilic compounds. Macromolecules such as plasmind DNA and fluorescent nanoparticles are encapsulated more efficiently than small molecule doxorubicin. (b) Cumulative DNA release from the nanocapsules in the absence of HFMF. The release rates of all three samples are very slow: over 10 days only 10–25% encapsulated DNA are released. At this time, the determining factors of the different release rates of the three samples are not known and deserve additional investigations. (c) HFMF-induced DNA release from nanocapsules. During the short experiment period, DNA release is negligible without magnetic field triggering (black curve). The release rate can be significantly increased if HFMF is applied. When the pulsed magnetic field is set at 0.8 or 1.2 kA/m (blue and green), the NCs release DNA in a burst-zero-burst fashion. When the pulsed field strength is increased to 2.0 kA/m (red), DNA release is enhanced when the field is on, and becomes appreciable even when the field is turned off. (d) Electrophoretic characterization of DNA structure after HFMF-induced release (left lane: molecular ladder; middle: original DNA; right: DNA released from NCs). The two bands in the middle and right lanes are likely due to DNAs with different 3-D

NIH-PA Author Manuscript

NIH-PA Author Manuscript

NIH-PA Author Manuscript

conformation. As shown in the gel image, DNA molecules released from the NCs share the same mobility with the original DNA sample, suggesting that the DNA molecules remain intact. (e & f) Cumulative pyrene release profiles in the absence or presence of HFMF. The overall trends for hydrophobic compound release with or without HFMF are similar to those for hydrophilic compounds, but the total amounts released are significantly less.

NIH-PA Author Manuscript
NIH-PA Author Manuscript
NIH-PA Author Manuscript

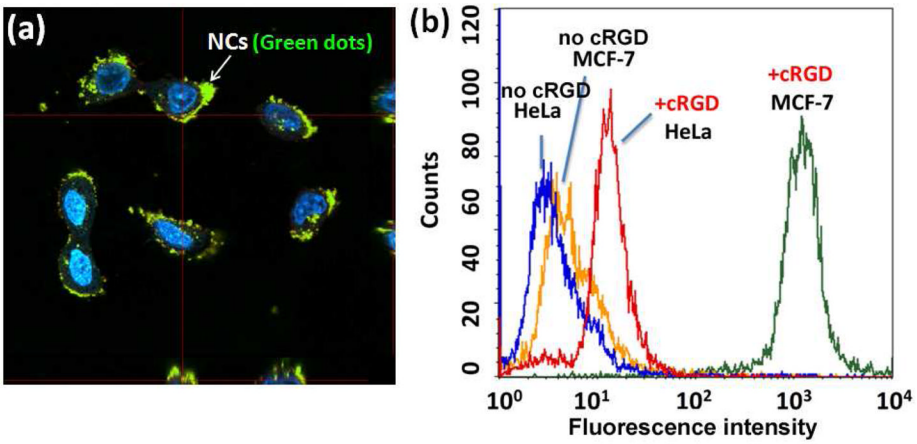

Figure 4.

Delivery of nanocapsules to cells *via* integrin targeting. (a) Laser-scanning confocal fluorescence imaging of MCF-7 cells treated with RGD-targeted NCs. After 24 h incubation, bright fluorescent signals are observed inside the cells. The fluorescent signals appears to have a punctuate pattern that often indicating endosome trapping. But at the current imaging resolution without endosome stained in a different color, the exact intracellular location and the integrity of endosome membrane cannot be determined. (b) Flow cytometry histograms of MCF-7 and HeLa cells after incubation with targeted and untargeted NCs for 4 hours. Compared with the control groups (MCF-7 cells treated with non-targeted NCs, HeLa cells treated with targeted, and non-targeted NCs), MCF-7 cells treated RGD-targeted NCs show > 100x intracellular fluorescence signals on average.

NIH-PA Author Manuscript

NIH-PA Author Manuscript

NIH-PA Author Manuscript

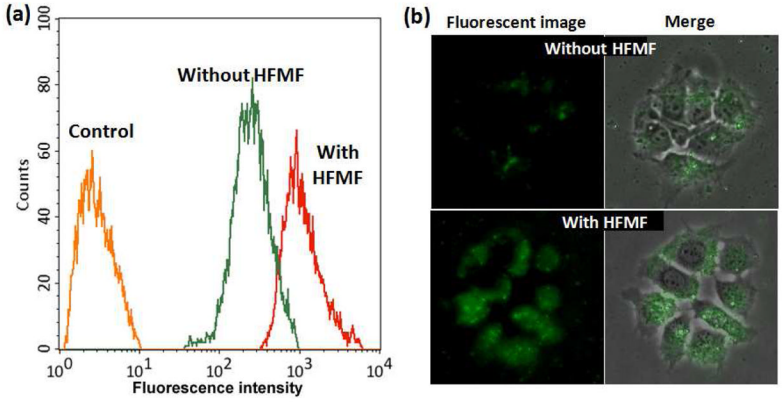

Figure 5.

HFMF-induced cargo DNA release in cells. (a) Fluorescence histograms of MCF-7 cells without incubation with NCs (orange), incubated with NCs (green) for 4h, and incubated with NCs for 4h and exposed to HFMF (2.0 kA/m) for 2 min (red). (b) Fluorescence microscopy of MCF-7 cells incubated with NCs before (upper panels) and after (lower panels) HFMF treatment. Upon exposure to HFMF, the fluorescence from FITC-DNA show a 5–6 fold increase in intensity. Note that the NCs stay inside cells for approximately 5 h total. Based on Figure 3, without HFMF the passive release of DNA should be at very low level over the 5 h period.

NIH-PA Author Manuscript
NIH-PA Author Manuscript
NIH-PA Author Manuscript

Table 1

Formulations of nanocapsule synthesis and size characterizations.

Sample	Fe_3O_4 (mg)	Copolymer (mg)	Oleic Acid (μL)	$W_{Fe_3O_4}/W_{polymer}$	Diameters (nm)
B60	12	20	2	60/100	265
B45	9	20	1.5	45/100	263
B30	6	20	1	30/100	295
B15	3	20	0.5	15/100	284
B7	1.5	20	0.25	7.5/100	294
B3	0.75	20	0.12	3.7/100	288